Electronic Supplementary Information

MXene/WS_2 2D/2D hybrid films for visible-light-activated NO_2 sensing at room temperature

Yi Xia [a, b], Sufang He [b], Junming Wang [b], Liexing Zhou [b], Jing Wang [c, *], Sridhar Komarneni [d, *]

[a] The Key Laboratory of Unconventional Metallurgy, Ministry of Education, Faculty of Metallurgical and Energy Engineering, Kunming University of Science and Technology, Kunming 650093, China

[b] Research Center for Analysis and Measurement, Kunming University of Science and Technology, and Analytic& Testing Research Center of Yunnan, Kunming 650093, China

[c] School of Chemical and Material Engineering, Jiangnan University, Wuxi 214122, China

[d] Department of Ecosystem Science and Management and Materials Research Institute, 204 Energy and the Environment Laboratory, The Pennsylvania State University, University Park, PA 16802, USA

1. Experimental

1.1. Materials Preparation

Chemical exfoliation method was applied to fabricate the 2D WS_2 nanosheets, which was conducted as follows: 15 mL hexane containing 2.0 M n-butyl lithium (Aladdin) and 0.8 g WS_2 powder (Sigma-Aldrich) were mixed in a conical flask with a volume of 30 mL, and the above mixture was stirred magnetically in a glove box filled with argon for 48 h. Thereafter, ethane was used to wash the above suspension for several times. The washed material was then filtered and dried in vacuum to obtain the intermediate product of Li_xWS_2. 100 mL water was used to initially disperse 0.5 g Li_xWS_2 prepared above, followed by an ultrasonic treatment for 60 min for full dispersion. After that, the 2D WS_2 nanosheets were obtained by centrifugation at 1500 r/min to remove the ~~massive~~ excess liquid.

* Corresponding authors. Email: jingwang@jiangnan.edu.cn (J. Wang); sxk7@psu.edu (S. Komarneni)

The 2D $T_3C_2T_x$ nanosheets were fabricated by the following procedure: 1 g of LiF was dissolved in 20 mL of 6 M HCl solution using a 100 mL polypropylene plastic bottle. Then 1 g of Ti_3AlC_2 was gradually added to the above solution and ~~kept~~ treated at 35°C for 24 h. After the reaction, the solid acid product was separated by centrifugation at 3500 r/min and washed with deionized water until the pH ~~value~~ was higher than 6. The dark green supernatant containing $T_3C_2T_x$ nanoparticles was obtained after centrifugation for 1 h, and its concentration was up to 1.5 mg/mL.

The $T_3C_2T_x/WS_2$ heterostructures were fabricated via a facile self-assembly route by mixing WS_2 ultra-thin nanosheets and $T_3C_2T_x$ nanosheets in methanol solution under vigorous ~~ly~~ stirring for 2 h at room temperature. Subsequently, the obtained product was filtered, washed, and stored in the mixed solution of deionized water and ethanol prior to characterization and gas sensing test.

1.2. Characterization

The microstructures of samples were studied by ~~a~~ high-resolution transmission electron microscopy (HRTEM, Tecnai G2 TF30, FEI, USA) and ~~a~~ field emission scanning electron microscopy (FESEM, Nova NanoSEM 630, FEI, USA). The structures of samples were investigated by powder X-ray diffraction (XRD) using Rigaku Dmax-2200 diffractometer, Japan) with CuKα radiation and ~~an~~ X-ray photoelectron spectroscopy (XPS) using PHI-5300 instrument, Philadelphia, USA. The photo-response performances of different sensors were examined by a digital source-meter (Keithley 2614B, Tektronix, USA) with 1 V voltage at 25°C. The photoluminescence (PL) spectra of samples were obtained on a luminescence spectrometer (F-7000, Hitachi, Japan) at room temperature equipped with a Xe lamp of 325 nm excitation.

1.3. Gas sensor fabrication and sensing performance tests

In this work, (100) N-type silicon wafer was used as the sensing substrate, on the surface of which was a thermally grown SiO_2 substrate with the thickness of 300 nm. Interdigital electrodes with both finger width and gap width of 10 mm fabricated by photolithography were spun by the WS_2-based suspension, and then dried at 90°C for 2 h. The homemade chamber used dry air as the carrier gas with the airflow of 200 mL/min and adjustable humidity from 0% to 80%, in which the obtained sensors were located and tested. The visible light was provided by an LED lamp with a Y-43 cut-off filter ($\lambda > 420$ nm). The current change of sensor was recorded by digital source-

meter at 25°C.

The response of a sensor is calculated as $\frac{I_g - I_a}{I_a} \times 100\%$, in which I_g and I_a are the film currents in studied gases and air, respectively. The response/recovery time refers to the time from the sensor contacting the measured gas to the current reaching 90% during response/recovery process.

2. Results and discussion

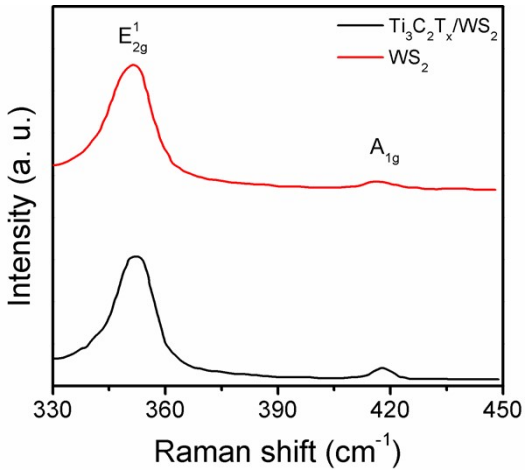

Fig. S1. Raman spectra of WS2 and i3C2Tx/WS2

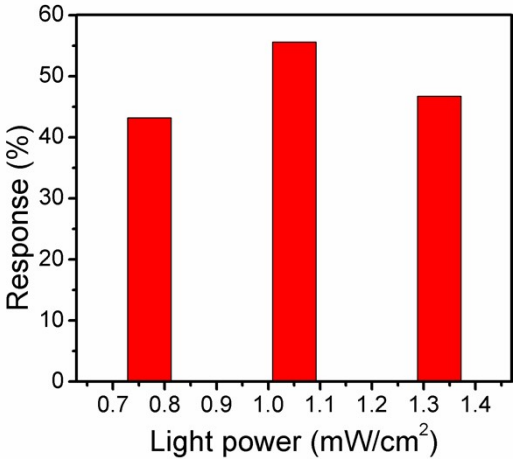

Fig. S2. Sensing responses of $Ti_3C_2T_x/WS_2$ based sensors under different light intensity ($mW \cdot cm^{-2}$).

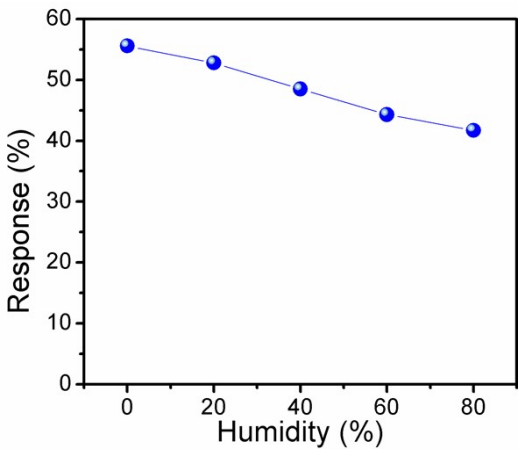

Fig. S3. Sensing response of $Ti_3C_2T_x/WS_2$ based sensors under different humidity under visible illumination.

Table S1. Comparison of NO_2 sensing performances between the developed sensor presently and reported NO_2 sensors based on various nanostructures and nanohybrids.

Sensing material	Temperature (℃)	NO_2	Response (%)	Response/recovery (s)	Ref.
WS_2/graphene aerogel	180	2 ppm	10	100/300	1
WS_2/Ag	100	500 ppm	16	＞500/＞600	2
Ultra-thin WS_2 nanosheets	RT	5 ppm	36.9	~100/~200	3
$WS_{2x}Se_{2-2x}$	RT	100 ppm	1067	＞300/＞1800	4
WS_2 Nanoplates	RT	5 ppm	48.2	＞400/＞1000	5
WS_2-carbon nanofiber	RT	1 ppm	15	＞300＞900	6
WS_2/ZnS heterostructures	RT	5 ppm	32.5	4/1000	7
MoS_2@WS_2 heterojunction	RT	50 ppm	27	1.6/27.7	8
WS_2/rGO (purple blue light)	RT	1 ppm	65	＞1200/＞1800	9

$Ti_3C_2T_x/WS_2$ (visible light)	RT	2 ppm	55.6	56/53	This work

Reference

[1] Yan, W., Worsley, M. A., Pham, T., Zettl, A., Carraro, C., & Maboudian, R.. Effects of ambient humidity and temperature on the NO_2 sensing characteristics of WS_2/graphene aerogel. *Applied Surface Science*, *450* (2018) 372-379.

[2] Ko, K. Y., Song, J. G., Kim, Y., Choi, T., Shin, S., Lee, C. W., & Kim, H. Improvement of gas-sensing performance of large-area tungsten disulfide nanosheets by surface functionalization. *ACS Nano*, 10 (2016) 9287-9296.

[3] Xu, T., Liu, Y., Pei, Y., Chen, Y., Jiang, Z., Shi, Z., & Li, X.. The ultra-high NO_2 response of ultra-thin WS2 nanosheets synthesized by hydrothermal and calcination processes. *Sensors and Actuators B: Chemical*, *259* (2018) 789-796.

[4] Ko, K. Y., Lee, S., Park, K., Kim, Y., Woo, W. J., Kim, D., & Kim, H.. High-Performance Gas Sensor Using a Large-Area $WS_{2x}Se_{2-2x}$ Alloy for Low-Power Operation Wearable Applications. *ACS applied materials & interfaces*, *10* (2018) 34163-34171.

[5] Koo, W. T., Cha, J. H., Jung, J. W., Choi, S. J., Jang, J. S., Kim, D. H., & Kim, I. D.. Few-Layered WS_2 Nanoplates Confined in Co, N-Doped Hollow Carbon Nanocages: Abundant WS_2 Edges for Highly Sensitive Gas Sensors. *Advanced Functional Materials*, *28* (2018) 1802575.

[6] J.-H. Cha, S.-J. Choi, S. Yu, I.-D. Kim, 2D WS_2-edge functionalizedmulti-channel carbon nanofibers: effect of WS_2 edge-abundant structure on25◦C NO_2 sensing, J. Materials Chemistry A 5 (2017) 8725–8732.

[7] Han, Y., Liu, Y., Su, C., Wang, S., Li, H., Zeng, M., & Yang, Z.. Interface engineered WS_2/ZnS heterostructures for sensitive and reversible NO_2 room temperature sensing. *Sensors and Actuators B: Chemical*, *296* (2019) 126666.

[8] Ikram, M., Liu, L., Liu, Y., Ma, L., Lv, H., Ullah, M., & Shi, K.. Fabrication and characterization of a high-surface area MoS_2@WS_2 heterojunction for the ultra-sensitive NO_2 detection at room temperature. *Journal of Materials Chemistry A*, *7* (2019) 14602-14612.

[9] Paolucci, V., Emamjomeh, S. M., Ottaviano, L., & Cantalini, C.. Near room temperature light-activated WS_2-decorated rGO as NO_2 gas sensor. *Sensors*, *19* (2019) 2617.